

Document downloaded from:

<http://hdl.handle.net/10251/168487>

This paper must be cited as:

Pastor, JV.; García Martínez, A.; Mico Reche, C.; Garcia-Carrero, AA. (2020). Experimental study of influence of Liquefied Petroleum Gas addition in Hydrotreated Vegetable Oil fuel on ignition delay, flame lift off length and soot emission under diesel-like conditions. *Fuel*. 260:1-11. <https://doi.org/10.1016/j.fuel.2019.116377>



The final publication is available at

<https://doi.org/10.1016/j.fuel.2019.116377>

Copyright Elsevier

Additional Information

# **Experimental study of influence of Liquefied Petroleum Gas addition in Hydrotreated Vegetable Oil fuel on ignition delay, flame lift off length and soot emission under diesel-like conditions**

## **Authors:**

José V. Pastor, A. García, C. Micó, Alba A. García-Carrero

## **Corresponding author**

José V. Pastor

CMT - Motores Térmicos / Universitat Politècnica de València. Camino de Vera s/n. 46022-Valencia (Spain)

[jpastor@mot.upv.es](mailto:jpastor@mot.upv.es)

## **Abstract**

The fundamental behaviour on ignition and combustion characteristics of blends of Hydrotreated Vegetable Oil and Liquid Petroleum Gas was investigated in a constant high pressure, high temperature combustion chamber, using a prototype lab-scale injection system adapted from a conventional common-rail system to conduct the injection events, ensuring that fuel was liquid at any point of the injection system and avoiding the formation of fuel vapour bubbles that could alter the injected fuel behaviour.

The ignition delay, flame lift-off length and the soot formation were studied by means of high-speed imaging techniques, for different operating conditions. The aim of the work is to characterize the effect of Hydrotreated Vegetable Oil-Liquid Petroleum Gas blend ratios on the previously mentioned parameters.

Experimental results show that the behaviour of the fuel blends follow the expected trends of conventional diesel type fuels when varying ambient temperature, density and injection

pressure. Hydrotreated Vegetable Oil, being the highest reactivity fraction, controls auto ignition of the blend. However, Liquid Petroleum Gas acts as combustion inhibitor increasing both ignition delay and lift-off length as its ratio in the blend increases. As a consequence, the differences observed in terms of flame radiation suggest that increasing Liquid Petroleum Gas fraction reduces soot formation as it promotes a higher air/mixture.

## **Keywords**

Hydrotreated Vegetable Oil., Liquefied Petroleum Gas, Dual fuel, Soot formation.

## **Abbreviations**

ASOI: After Start of Injection

ECN: Engine Combustion Network

FWHM: Full Width at Half Maximum

GCI: Gasoline Compression Ignition

HCCI: Homogeneous Charge Compression Ignition

HD: High Density

HPHT: High Pressure and High Temperature Installation

HRF: High Reactivity Fuel

HVO: Hydrotreated Vegetable Oil

ID: Ignition Delay

LD: Low Density

LOL: Lift-off Length

LPG: Liquid Petroleum Gas

LRF: Low Reactivity Fuel

LT: Low Temperature

LTC: Low Temperature Combustion

NL: Natural Luminosity

NO: Nominal Operation

$O_{2\text{ amb}}$ : Oxygen concentration in the chamber

$P_{\text{amb}}$ : Pressure in the chamber

$P_{\text{inj}}$ : Injection pressure

PPCI: Partially Premixed Compression Ignition

RCCI: Reactivity Controlled Compression Ignition

SOC: Start of Combustion

SOI: Start of Injection

$T_{\text{amb}}$ : Temperature in the chamber

$\rho_{\text{amb}}$ : Density in the chamber

$\rho_{\text{fuel}}$ : Fuel Density

## **Acknowledgements**

The authors acknowledge that this research work has been partly funded by the Government of Spain and FEDER under TRANCO project (TRA2017-87694-R) and by Universitat Politècnica de València through the Programa de Ayudas de Investigación y Desarrollo (PAID-01-18) program.

## **1 Introduction**

The transport sector represents nowadays around 20% of the total Green House Gases emissions [1]. Thanks to the stringent limitations applied since 1990, the pollutant emissions such as carbon dioxide are targeted to be reduced progressively until today. Following the current trend from now to 2050, emissions from the transport sector can be reduced by more than 60% with respect to levels reached in 1990. Compared to more recent data, in 2030 emissions are expected to decrease by 20% with respect to 2008 levels [1]. In order to meet current

environmental pollution and emission regulations, researchers are always seeking for different solutions to decrease Particulate Matter (PM), CO<sub>2</sub> and NO<sub>x</sub> emissions.

One of the main research topics in this regard is the use of alternative fuels. More specifically, the use of biofuel has shown up as a potential alternative. Several results found in the literature show that a biodiesel [2] or even different biodiesel-diesel blends [3] offer the similar efficiency as pure diesel while reducing CO<sub>2</sub>. In terms of soot emissions, Hydrotreated Vegetable Oil (HVO) has shown great potential in soot reduction, around 50 and 60 % when tested in a single cylinder engine in comparison to conventional diesel. That could be due to its almost aromatic-free composition [4]. On the other hand, Liquefied Petroleum Gas (LPG) was also studied in a compression ignition engine and it showed reductions in soot emission compared to base line diesel in dual fuel operation [5]. Although LPG comes from fossil sources while HVO comes from natural lipids (vegetable oils and animal fats), both could have a great potential in reductions of emissions levels.

HVO is produced by an alternative esterification process called a Hydrotreating. This process is characterized by reducing oxygen, sulphur, nitrogen and aromatics while enhancing the cetane number, density and smoke point that avoid detrimental effect produced by ester-type biodiesel fuels [6]. HVO has similar chemical characteristics to diesel [7] but in comparison, it presents a better behaviour in terms of spray characteristics and emission levels. Even NO<sub>x</sub>, CO<sub>2</sub> and PM concentration can be reduced if HVO is used [8], [9]. On the other hand, regarding LPG, it has been tested in internal combustion engines offering promising results in terms of unburned Hydrocarbons, CO and other pollutant emissions [10], [11],[12]. However ignition quality is the main drawback that can be solved with the addition of cetane improvers achieving commercial diesel fuel levels [13].

Another way to approach the more and more stringent pollutant emission scenario has been the development of new combustion concepts, focused on reducing engine-raw emissions while keeping good engine performance. More specifically, the promotion of Low Temperature Combustion (LTC) and air-fuel premixed combustion conditions has shown big potential, in this regard Homogeneous Charge Compression Ignition (HCCI), Partially Premixed Compression Ignition (PPCI), Gasoline Compression Ignition (GCI), Reactivity Controlled Compression Ignition (RCCI) are some of the most relevant LTC strategies that can be found in literature. LTC strategies mitigate the NO<sub>x</sub> and soot formation by promoting a highly diluted in-cylinder fuel-air mixture and extended premixing time between fuel and air prior to combustion [14], which breaks the NO<sub>x</sub>-soot trade-off with conventional diesel combustion strategies. Additionally, the gross indicated efficiency would not be affected while CO and unburned HC decrease as well as the efficiency of the engine is improved due to the heat transfer reduction, among other factors [15],[16].

RCCI, in particular, is one of the leading concepts. It is based on controlling the combustion process and adapting to different engine loads by tailoring the mixture reactivity inside the combustion chamber. This is achieved by using two different reactivity fuels, defined as low reactivity fuel (LRF) and high reactivity fuel (HRF) respectively. Usually, the LRF is injected at low pressures with a port fuel injector while the HRF is directly injected into the cylinder at high pressures [15], [17] However, it is also possible to find applications where fuels were mixed prior to their injection, which ends with the need of two independent injections system and facilitates its application.

Considering all above mentioned, this study aims to combine the RCCI dual fuel combustion concept with the use of alternative fuels. HVO is defined as the HRF and LPG as the LRF. The blend of both is stored in the same tank and injected through a common injection system. The main objective is to evaluate under controlled ambient conditions the performance and soot

emissions of fuel blends of liquid (HVO) and gaseous fuels (LPG) with potential to be used for RCCI dual fuel combustion in compression ignition engines for heavy duty transport. Thus, auto ignition, flame structure and soot formation are studied by means of high speed imaging techniques in a high pressure and high temperature combustion rig. The details of the experimental hardware used is presented in the next section, followed by the discussion of results, which emphasizes the effect of fuel composition in the evolution of the spray and fuel combustion, as well as soot formation.

## **2 Experimental Methodology**

Different blends of HVO and LPG have been injected into a high pressure and high temperature environment using a common-rail injection system which was modified to allow handling of the fuel blends and ensuring that evaporation in the injection system was avoided. The analysis of the effect of fuel composition on the ignition, flame development and soot emissions is made by applying three simultaneous high speed imaging techniques: Schlieren imaging, broadband natural flame luminosity (NL) and high speed OH\* chemiluminescence imaging. The following paragraphs describe first the test facility, the injection system and the characteristics of the fuels used. Then, the test matrix and finally the experimental techniques used are described, with emphasis on the experimental procedures followed for the measurement and analysis.

### **2.1 High-Pressure & High-Temperature facility**

The experiments have been performed in a high-pressure, high-temperature facility (HPHT). The pressure, temperature and composition of the gas in the vessel can be controlled independently, to achieve pressures of up to 15 MPa, temperatures of up to 1100 K and oxygen concentration between 0 and 21% by mixing air with pure nitrogen. In this way, it is possible to mimic thermodynamic conditions existing in any real internal combustion engine at the moment of fuel injection, with a homogeneous temperature field in the area of study, and free

of the uncertainties associated to engine transients, whilst providing wide optical access for the application of several techniques. As shown in Figure 1, the facility can operate in open loop with air or as a closed loop circuit to reduce O<sub>2</sub> concentration. The regulation and control system allows ensuring stable thermodynamic conditions and composition for long time periods so that many injection and combustion events can be recorded, which ensures statistical reliability of the results obtained. Moreover, to ensure that any temperature transients generated locally by the combustion under study are avoided, injection is performed at low frequency (1 injection shot every 4 seconds). The boundary conditions have been characterized in detail and a complete description of the facility is given in [18].

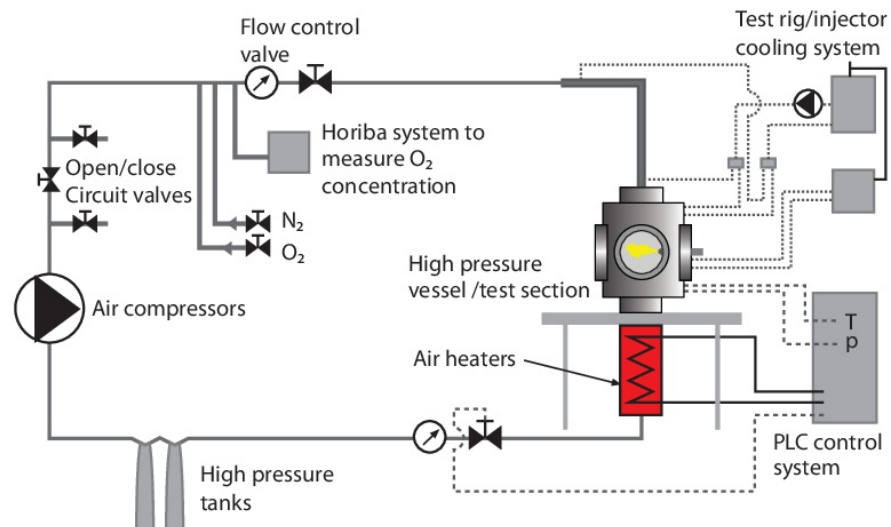


Figure 1. Scheme of the High-Pressure and High-Temperature facility.

## 2.2 HVO- LPG Injection system

A modified injection system based on a conventional common-rail system was used to inject fuel into the combustion vessel as sketched in Figure 2. Considering that LPG is a gas at atmospheric pressure and room temperature, and that common-rail injection systems are designed to operate with liquid fuels, it was necessary to ensure that fuel was liquid at any point in the hydraulic circuit. For this purpose, conventional fuel tanks for automotive LPG cars were filled in with the desired blends of HVO and LPG at a pressure of 7 bar. Fuel delivery to the



rest of the circuit, i.e. to the common-rail system, was made by activating the low pressure pump inside the fuel tank. The rest of the injection system components are standard and include the high-pressure pump, a common rail with pressure regulator controlled by a PID system, and piezoelectric injector. In addition, an special injector holder is used to keep constant the injector tip temperature at the desired value through the whole test matrix [19].

To ensure that fuel was liquid at any point of the injection system avoiding the formation of fuel vapour bubbles that could alter the injected fuel behaviour, two heat exchangers were used as shown in Figure 2. One of them was set just downstream of the pressurized fuel tank, before the high-pressure pump of the common-rail system. The second was set at the fuel return pipes to ensure that fuel was cooled down prior to drive it back to the pressurized tank. Both of them were instrumented to monitor pressure and temperature at any moment ensuring tests repeatability.

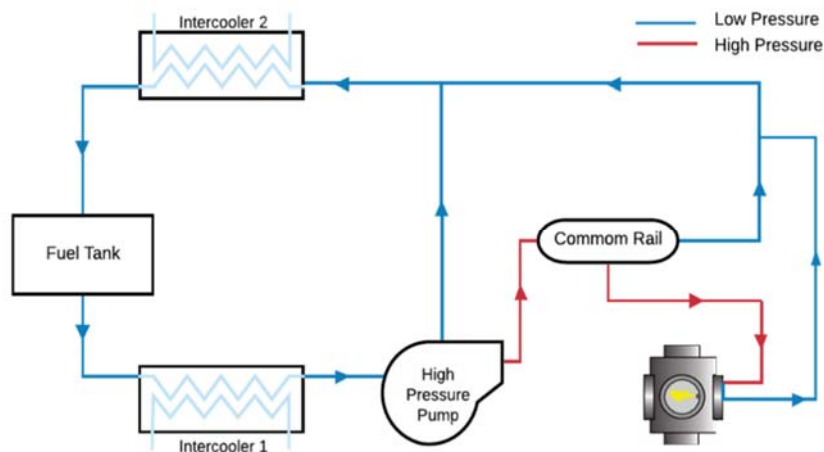


Figure 2. High pressure injection system for HVO- LPG blends.

In addition, to avoid any fuel leakage of gas to the laboratory atmosphere, both fuel returns from the high-pressure pump and from the injector were communicated and driven back to the tank. Besides, this allows to ensure that, due to the low amount of fuel injected during these

tests, the composition of the fuel blend in the tank remained unchanged. All the low-pressure part of the hydraulic system was set to 7 bar and 290 K.

To perform a detailed characterization of the spray and combustion enhancing fuel effects a single hole nozzle was used, so that isolated sprays were imaged. The nozzle used is a single-hole one with a 140  $\mu\text{m}$  outlet diameter, a 1 mm long hole thickness and with a conical shape (K factor of 1.5). It has been used for some other studies by the authors during the last years [20], [21].

## 2.3 Fuels and Test Matrix

### 2.3.1. Fuels properties

Four different fuels have been considered in this study as representative substitution rates in a hypothetical dual fuel combustion mode in a compression ignition engine. Pure HVO is considered as the High Reactivity Fuel (HRF) of the dual fuel combustion mode with a Derived Cetane Number close to conventional diesel fuel, LPG being the Low Reactivity Fuel (LRF). Thus, pure HVO is considered the reference fuel in this study and represents the zero substitution rate of the dual fuel mode. Then, three blends of HVO and LPG with percentages of LPG of 25%, 50% and 75% in mass are considered to represent different rates of substitution.

The main properties for the two components of the blend, HVO and LPG, are detailed in Table 1. All along the document, the four fuel are identified as “HVO” for pure HVO, and “7525”, “5050” and “2575” for the blends with 75%, 50% and 25% of HVO respectively.

Table 1. Fuel properties.

Characteristics	HVO	LPG
Density [ $kg/m^3$ ]	779.1	502
Viscosity [ $mm^2/s$ ]	2.7	0.0074

Lower heating value [ $MJ/kg$ ]	44	45.79
Vapour Density [ $kg/m^3$ ]	3.4	$2.48 \times 10^3$
Vapour Pressure [bar]	0.87	15
Boiling Point [ $^{\circ}C$ ]	(180)-(320)	(-42.1)-(3.7)
Flash Point [ $^{\circ}C$ ]	>55	(-107.5)-(-101.6)
Autoignition [ $^{\circ}C$ ]	338	>400
Derived cetane number (IQT)	70.9	--

### 2.3.2. Operating conditions

For the four fuels, a set of parametric studies has been performed. Ambient density and ambient temperature were set as variables, as well as oxygen content and injection pressure. The injection strategy used was a single injection with an energizing time of 1500  $\mu s$ , which provides an injection event long enough to study the development of the spray and flame under mixing controlled combustion. The fuel mass flow rate was 0.00381  $kg/s$

Four ambient conditions have been considered in the base test matrix summarized in Table 2: Low Density (LD), Nominal Operation (NO), High Density (HD), and Low Temperature (LT). They have been considered as representative of LTC conditions, where dual fuel combustion has higher potential. Starting from a nominal operation (NO) with 22.8  $kg/m^3$  air density, a variation of temperature (800 and 900 K) at constant density and a variation of density (from 15.2 to 30.4  $kg/m^3$ ) at constant temperature were performed. In all cases, two rail pressures of 500 bar and 1000 bar were considered.

In addition, two specific test conditions were included to complete the test matrix. On the one side, tests under inert conditions were carried out to verify that the spray development was not affected by the fact that LPG has a high saturation pressure as is shown in Table 1.

Table 2. Test Matrix.

	T [K]	$\rho$ [kg/m <sup>3</sup> ]	O <sub>2</sub> [%]
Low Density (LD)	900	15.2	21
Nominal Operation (NO)	900	22.8	21
High Density (HD)	900	30.4	21
Low Temperature (LT)	800	22.8	21

## 2.4 Optical set up

Aiming to analyse the effect of the LRF substitution rate upon spray development, ignition and soot formation, three different optical techniques have been applied simultaneously using the two opposed optical access windows in the vessel, trying to maximize the amount of information obtained. A sketch of the optical arrangement is shown in

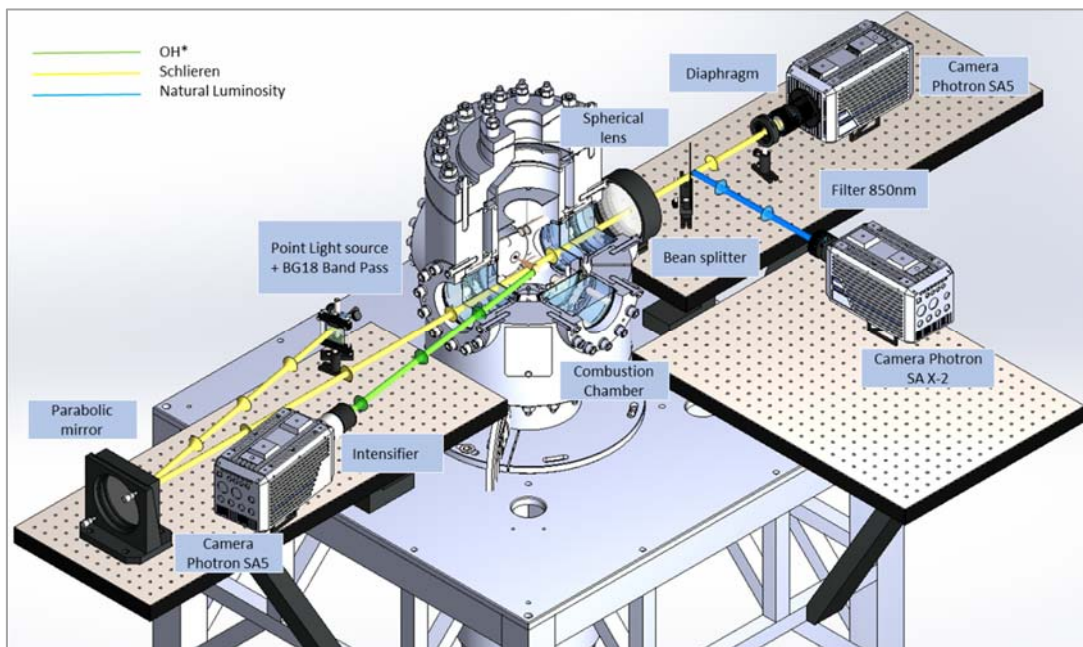


Figure 3.

Figure 3. Scheme for three optical technique used in the tests.

### 2.4.1 *Schlieren visualization*

The Schlieren technique is based on the deviation suffered by a light beam, due to refraction, when crossing a media with refractive index gradients [22]. Consequently, it allows recording as an image any variations of refractive index, such as those produced by the injection of fuel spray in liquid and vapour phases, as well as the density variations provoked locally by the fuel auto ignition or flame development.

A high-speed, single-pass Schlieren imaging setup, very similar to that described in detail in [23] was used to detect the spray and flame boundaries at any operating conditions. A scheme of the optical arrangement is shown in

Figure 3. A diffused point light obtained from a Xenon arc lamp with a liquid light guide and a pinhole was collimated by a parabolic mirror ( $f=610\text{mm}$ ) which directs it through the combustion chamber. In addition, a BG18 band pass filter is used to restrict the spectrum of the Xenon lamp and avoid interference in the NL images commented later. A spherical lens ( $f=450\text{mm}$ ) was placed on the other side of the chamber to focus the light onto a so-called Fourier plane, where a diaphragm was located with a cut-off diameter of 3 mm just before the high-speed camera (Photron Fastcam SA-5) equipped with a Carl Zeiss Makro-Planar T 100mm  $f/2$  ZF2 camera lens. Images were recorded at a fixed frequency of 20 kfps, with a constant shutter time of  $2.5\ \mu\text{s}$ , a total magnification of 11 pixel/mm and a resolution of  $1024 \times 368$  pixel. A minimum of 30 injection cycles per test were recorded in any case.

The Schlieren images have been used to depict a global phenomenological description of the injection and combustion process of the different fuel blends, which will be presented later. In addition, due to the fair space and time resolution of the Schlieren recordings, these images were also used to determine the real Start of Injection (SOI) for every case with sub-interframe temporal resolution. This was done by extrapolating the spray tip penetration measurable in the

first injection frames to estimate the exact instant when fuel starts to exit from the nozzle hole. This SOI is used in all the results presented in this paper as the temporal origin of any measured parameter with any cameras, since the three cameras used the same trigger signal.

As for the spray and combustion parameters measured from the Schlieren images, segmentation from the background is performed by applying the methodology described by Siebers [24], which has become a standard in the Engine Combustion Network [25]. Once the boundaries are determined, the spray tip penetration is measured as the higher distance to the nozzle on the spray axis at any moment. The same criterion is used to determine the flame penetration after ignition takes place. The ignition event can be tracked with this technique too, both spatially and temporally. As it can be found in literature [24], the first stage of the auto ignition process, also called the cool flame stage, makes the spray contrast of the Schlieren images to vanish. The second stage, i.e. the high temperature ignition stage, provokes spray radial expansion and spray tip acceleration [26] and the local increase of temperature enhances again the contrast in the images. Using these observations, the timing when ignition occurs can be determined from the Schlieren movies by evaluating the evolution of the accumulated intensity of the spray in the Schlieren images, after segmentation, as described in [24]. Figure 4 shows a plot of the accumulated intensity increment between consecutive frames for one of the cases analysed in the current paper. The regression of the spray intensity increment reveals the occurrence of the cool flame, which is followed by a step increase associated to the occurrence of the high temperature ignition stage. In this paper, the ignition timing has been determined as the mean value between the cold flame minimum and the easily detectable maximum after ignition. With this criterion, the ignition times measured are much more suited to the ignition times observed in the images collected in the experiments than with the criterion used in [27] where the ignition delay is chosen as the time where the maximum intensity increment occurs. It was observed

here that at the time when the maximum intensity increment occurs, the jet has already widened showing that the combustion process has started moments before.

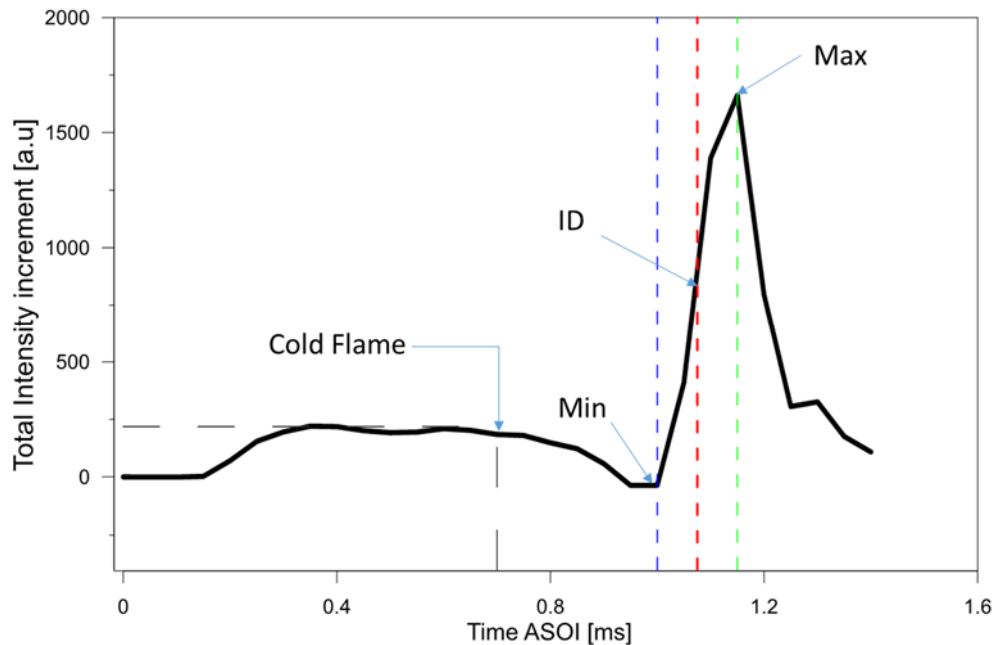


Figure 4. Description of method used to define Ignition delay. Total intensity increment correspond to blend 7525 at LD condition and 500 bar of injection pressure.

#### 2.4.2 Natural Luminosity

Images of Natural Luminosity (NL) are normally considered as those registering the broadband radiation of the flame without using any particular optical filter [24]. In such cases, considering the spectral response of the camera, the light collected will be almost entirely the thermal radiation arising from small soot particles present in the flame, and in some cases can include a minor contribution of other types of chemiluminescence radiation too, which can become significant only in low sooting flames cases. Then, qualitative and topological description of the sooting flame evolution can be obtained, but no quantitative description of the combustion intensity is expected since this is a line-of-sight technique and consequently renders a variable that is integrated along the optical-path, so spatial resolution is only possible as two dimensional

distribution of the optical-path integrated variable. In this work, NL images are not images of flame broadband radiation, but of radiation at around 850nm (40nm FWHM) since an interference filter is used to avoid registering at the same time flame NL and the illumination light used for the Schlieren. As a consequence, the spectrum fraction is severely reduced as well as the light collected. However, the analysis is exactly the same as with conventional broadband NL images, since the only significant contribution of the flame in the near-IR spectrum comes from soot particles incandescence. It is well known that flame brightness does not depend only on soot concentration, but also on flame temperature [28]. However, for isolated sprays as those analysed in this work, if the only parameter changed is the fuel composition, it can be assumed that the temperature field in the flame at equivalent instants after ignition will not be too different. Thus, flame brightness can be a qualitative indicator of the amount of incandescent soot in the flame.

In this study, Natural Luminosity was recorded with a high-speed camera (Photron Fastcam SA-X2) at a fixed frequency of 20 kfps, with a resolution of 512x736 pixel, and a total magnification of 4.9 pixel/mm. Shutter time was adapted to the luminosity of each tested case to use properly the dynamic range of the camera. A minimum of 30 injection cycles per test were recorded in any case, too.

Two parameters have been derived to evaluate the influence of the fuel blend on soot production. On the one side the accumulated flame intensity, which is obtained by addition of the values of the grey levels of all the pixels in the image. It will provide information on the soot amount and flame size. On the other side, the average flame intensity is obtained as the ratio between this magnitude and the flame size, which is quantified as the number of pixels with a grey level higher than background mean level plus twice its standard deviation. This second magnitude takes into account the average soot concentration in the flame, independently of its degree of development at any moment.



### **2.4.3 *OH\** chemiluminescence**

OH\* radicals are known to be a good tracer of high temperature combustion regions in a flame [29], so that visualization of OH\*-chemiluminescence at the base of the flame makes it possible to quantify the Lift-Off Length (LOL). Additionally, if an intensified high speed camera is used, ignition delay can be measured, too.

In this work, a high speed image intensifier (Hamamatsu C10880), coupled to a high speed camera (Photron Fastcam SA5) with a 1:1 relay lens, equipped with a UV f/4 100mm focal length lens (OUC 2.50 by Bernhard Halle Nachfl.) was used. An interference filter centred at 310nm (10nm FWHM) was placed in front of the camera to remove most of the radiation of the flame while keeping OH\*-chemiluminescence. Images were taken at a fixed frequency of 15 kfps, with a resolution of 320x536 pixel, and a magnification of 3.4 pixel/mm. Shutter time was fixed in 33us and care was taken to ensure that light saturation, whenever occurred, did not affect the measurement of the LOL and was low enough as to not imply any risk for the intensifier safety. Again, at least, 30 valid injection cycles per test were recorded in any case, at least.

Ignition delay was computed determining the first frame with light intensity, as a check to confirm the results obtained with the Schlieren technique. As for the measurement of the LOL, the algorithm used is based on the Engine Combustion Network (ECN) recommended procedure described in [30], where the LOL was determined by finding the distances between the injector tip and the first axial locations above and below the spray centerline with intensity greater than 50% of the intensity peak of that zone.

## **3 Results and discussion**

Before entering into the detailed quantification on the effect that the HVO-LPG blend ratio has upon the spray features, the mixing process and soot formation, a phenomenological description

of the injection and combustion process is given, paying attention to the effects clearly linked to the fuel composition.

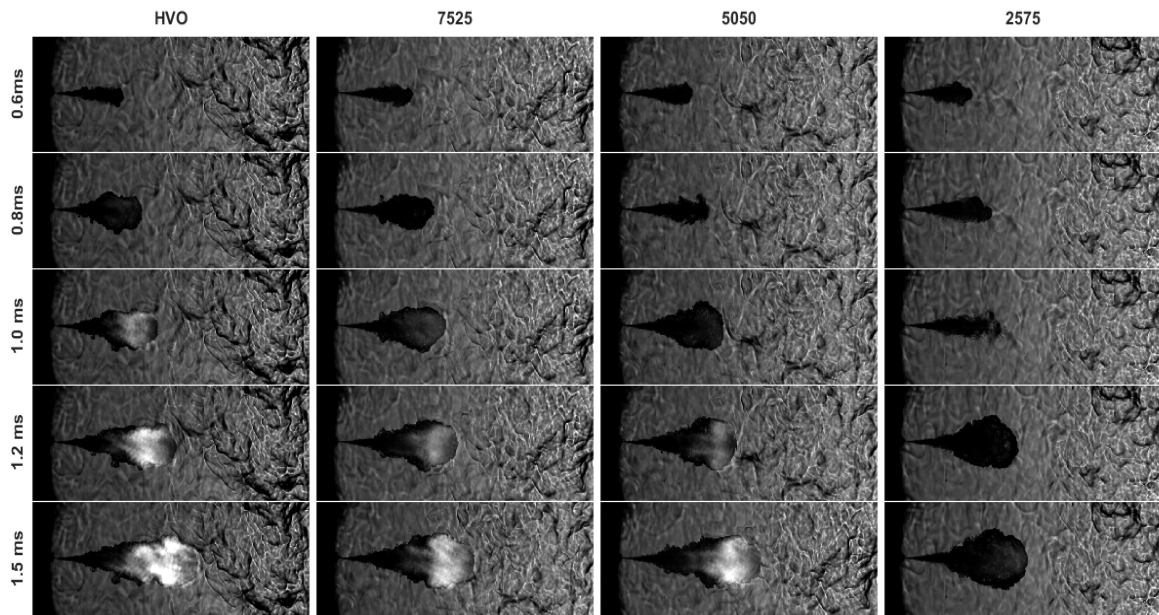


Figure 5. Combustion evolution for the four blends tested at Nominal conditions (NO) and injection pressure of 500 bar.

In Figure 5. Combustion evolution for the four blends tested at Nominal conditions (NO) and injection pressure of 500 bar. Some frames of the high-speed images recorded using the Schlieren technique are presented. These images show the evolution of the sprays and the combustion. The nozzle is located at the left hand side of the images and the sprays are injected at 500 bar into a nearly stagnant flow with constant and uniform temperature field of 900 K and  $22.8 \text{ kg/m}^3$  air density. Five frames have been selected to evidence the influence of the HVO-LPG ratio in the spray and flame development, before the end of the injection, i.e. when the spray is still mixing controlled. Images at the left column correspond to pure HVO, and the other three columns to the right are for increasing LPG proportion in the blend.

From top to bottom of any case the following events can be appreciated in the spray and flame development: in the first frames the spray in liquid or vapour phase appears as a dark shape that

tends to increase in size as time evolves. When the first stage of the auto ignition process occurs the spray contrast of the Schlieren images vanish (see, e.g. the third frame of the last column). Tip acceleration and radial expansion of the burning spray become evident in the following frame when high temperature ignition has already started. Certain time after ignition, incandescent soot appearance becomes evident and it can be seen as bright regions in the images.

Regarding the geometry of the spray, there are no significant differences before auto ignition for the 4 blends, which suggests similar characteristics of injection between the four fuels. However, two issues apparently linked to the ratio of LPG in the blend can be easily identified. First, ignition delay increases with LPG content in the blend, which indicates that LPG acts as an ignition inhibitor reducing burning propensity of HVO. A second effect is that the flame brightness decreases clearly when LPG rate increases, pointing out that LPG is a less sooting fuel than HVO. However, the Schlieren technique does not allow to perform the soot formation assessment. Although it is possible to appreciate the high luminosity of the HVO, it is necessary to use a specific optical technique to confirm which fuel has higher soot formation tendency. Therefore the Natural Luminosity technique has been used for this purpose.

In the next subsections, ignition delay and flame brightness effects will be quantified: first, auto ignition and macroscopic characteristics will be analyzed in terms of fuel effects on auto ignition, penetration and flame lift off length; then attention will be paid to soot formation.

### **3.1 Auto ignition and macroscopic characteristics**

#### ***3.1.1 Ignition Delay (ID)***

The ignition delay (ID) is defined as the time elapsed from the Start of Injection (SOI) and the Start of Combustion (SOC) and has been calculated from the Schlieren images following the procedure described in section 2.4.1. This technique was chosen for this purpose, instead of

high-speed OH\* chemiluminescence, because it was performed at a higher acquisition rate (better time resolution). Besides, both techniques were compared, and differences were below 0.05 ms, which could be due to the difference in time resolution of both techniques.

The influence of the different operating conditions upon the ignition delay has been widely studied in literature and a similar analysis will not be performed here. However, in order to check consistency of the experimental data of this work with the well-known spray physics, a comparison of the experimental data versus some correlations available in literature is given in Figure 6. In particular, the correlation by Benajes [31] obtained for n-dodecane and represented in Equation **¡Error! No se encuentra el origen de la referencia.**

$$ID^* \propto \exp\left(\frac{7523}{T_{amb}}\right) \cdot \rho_{amb}^{-1.35} \cdot (P_{inj} - P_{amb})^{-0.09} \cdot O_{2\% amb}^{-0.51} \quad 1$$

Where the constant inside the exponential term is related to the global activation energy of reactions. Equation 1 indicates that the ID is proportional to terms on the right. The correlation is completed with a constant term which reflects fuel properties contribution, and it will be not considered in this study, therefore the  $ID^*$  will be referred only to the proportionality. This correlation shows the effect of boundary conditions over the ignition delay [31], [32], which decreases with increasing the temperature, as it accelerates oxidation reactions. ID also decreases with increasing density and injection pressure, as both parameters enhance the mixing and evaporation processes. In Figure 6, operating conditions have been represented in ellipses with continuous lines

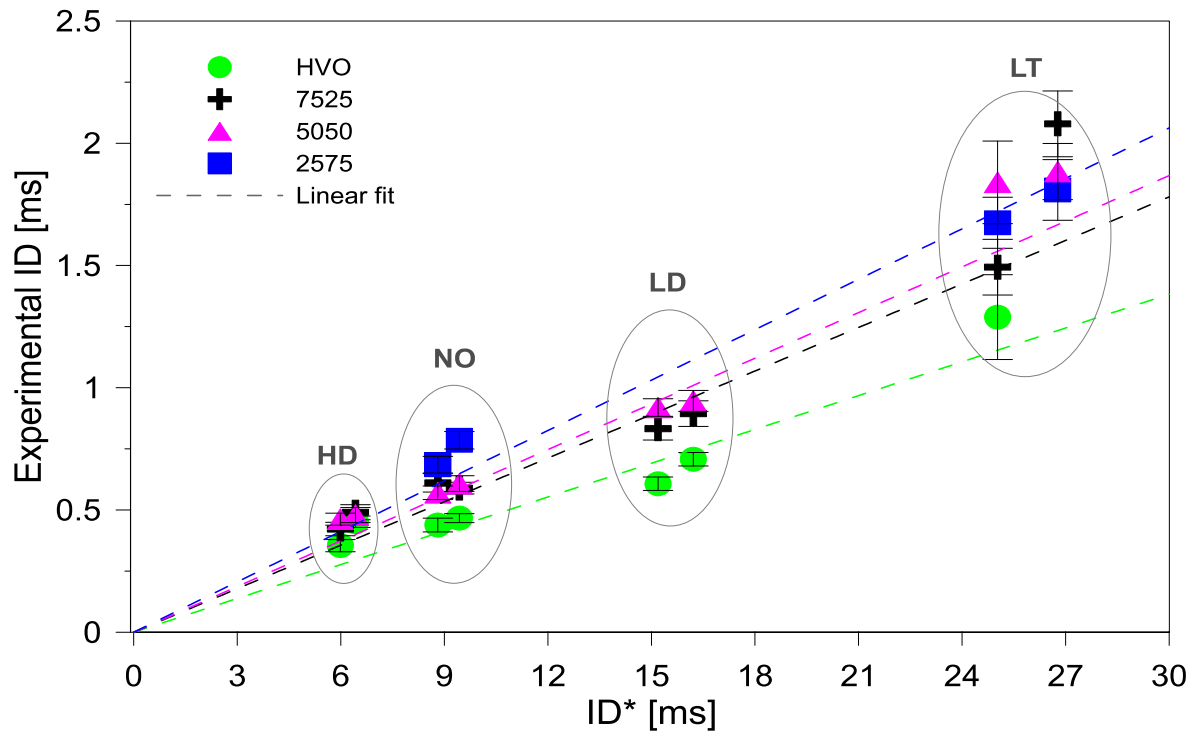


Figure 6. Comparison of current experimental data with correlation calculated by Benajes [27] for n-dodecane.

It is worth mentioning that the experiments in the work [31] were performed in the same facility as the present work, but using different fuel. In Figure 6 is represented the experimental ignition delay versus the theoretical ignition delay ( $ID^*$ ) obtained using the Equation; **Error! No se encuentra el origen de la referencia..** The slope obtained from linear fit (dashed lines) for each fuel corresponds to the missing constant in the equation 1. Based on these correlation and linear fit, in Figure 6 is observed that stratification exists by fuels, being the higher values of ID for HVO-LPG blends. HVO is the first to start combustion and the blend with the highest proportion of gas (2575) is the last. Thus, LPG clearly increases ignition delay compared to the HVO, independent of the ambient or injection condition. For  $15.2 \text{ kg/m}^3$  and:  $22.8 \text{ kg/m}^3$  ambient density ID of blends with low (7525) and medium (5050) LPG ratio increased between 26% and 34% with respect to HVO at 500 bar of injection pressure, but fuel 2575 (high LPG ratio) showed an increase of 68%. However, for  $30.4 \text{ kg/m}^3$  ambient density, the ID increase

for the three blends in comparison with HVO is only around 6% to 8%. For the cases at 1000 bar of injection pressure the differences increase, reaching up to 50% of difference respect to HVO in LD operating condition, and the difference increase up to 40% in the NO and HD condition for HVO-LPG blends. In the case of low temperature (800K), the differences between fuels vary from 15% and 40% for both injection pressure. For LT operating condition, the experimental data does not follow the linear correlation described by equation 1. The effect of boundary conditions in comparison to other experimental points is the same as described previously. However, blends show larger variations than the ones predicted by the correlation. Moreover, when ambient temperature reduces, the ignition delay increases as well as its statistical uncertainty. At low temperature case, with ID of the order of 2 ms, data scattering is higher in reference to other operating condition.

### 3.1.2 Spray tip penetration

Spray tip penetration and flame penetration were obtained from high-speed Schlieren images, as described in previous sections.

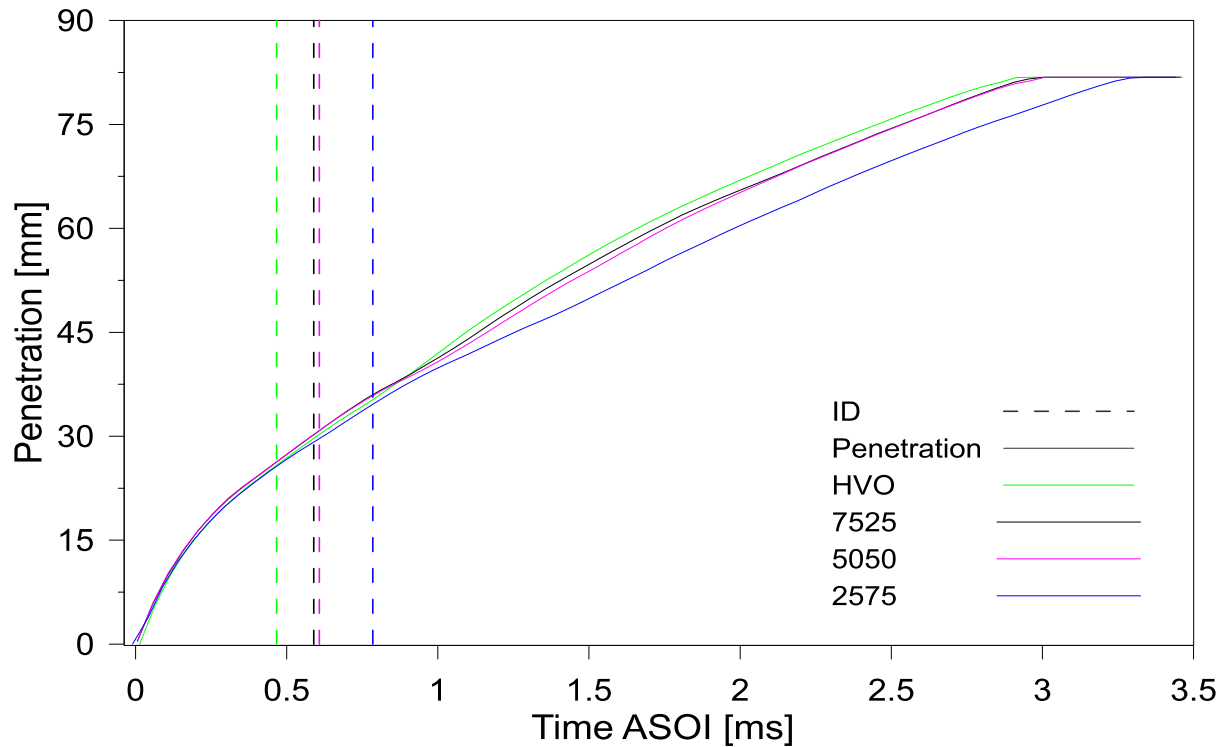


Figure 7. Temporal evolution for vapor penetration of each blend at  $T=900\text{K}$ ;  $\rho=22.8\text{ kg/m}^3$  and  $P_{inj}=500\text{bar}$ .

Figure 7 shows the temporal evolution of the vapor/flame penetration obtained for each blend at Nominal operating condition at 500 bar of injection pressure. It is possible to state that there is a first stage where vapor penetration is identical for all the blends (up to 0.48 ms) and, after a certain time (ignition time), some differences arise. This first stage corresponds to the ignition delay phase which extends for each blend until combustion starts, timing that has been marked in the graph as dashed vertical lines for each blend. During the period until ignition, attending to momentum flux conservation equations, there should be no effect of the fuel blends on the spray behavior as discussed in [33]; spray momentum flux at the nozzle orifice only depends

on the pressure drop across the nozzle and on the orifice area, and none of them change throughout the experiment.

It is worth mentioning that, despite the physical properties of the fuel blend (mainly density and viscosity) not affecting spray tip penetration (until ignition stage), density may affect the fuel injection rate (which is not relevant in these experiments with long injections) while viscosity is related with fuel behavior inside the injection system. Consequently, it influences the hydraulic delay of the injector and the real Start of Injection (SOI) occurs later with the increasing proportion of LPG. As explained in the methodology section, the real SOI was determined by means of the high-speed Schlieren images and all curves in this paper have been shifted accordingly to refer them always to real SOI.

Despite differences observed in the hydraulic delay, injection process is not affected by the different properties of LPG and HVO as it is confirmed by the similarities observed in fuel penetration before the start of combustion.

After ignition, the flame penetration curves depart from each other because of the flame expansion described in previous works [20]. Not characteristic effect associated to fuel composition was observed in these experiments, other than the fact that the shorter the ignition delay, the longer the flame penetration [34].

### ***3.1.3 Lift off length***

Flame lift-off length plays an important role in the combustion and soot formation processes, since it is strongly related with the quality of fuel-air mixing process upstream of the combustion region[32] [35]. Consequently, flame LOL is a parameter which is worthy to be studied in detail with these fuel blends.



As previously done with the Ignition Delay, a comparison of the raw experimental data obtained in this work with correlations available in literature is performed. The time interval to calculate the stable LOL was between 3.2 ms and 3.8 ms.

The correlation proposed by Benajes et al. [31] is shown in Figure 8. It was obtained for n-dodecane, in the same facility and under similar conditions to the ones in this work. This correlation is represented by Equation 2:

$$LOL^* \propto T_{amb}^{-3.89} \cdot \rho_{amb}^{-1} \cdot \left( 2 \cdot \frac{P_{inj} - P_{amb}}{\rho_{fuel}} \right)^{0.54} \cdot O_{2\,amb}^{-1} \quad 2$$

It is worth mentioning that in equation 2 a constant is missing, that converts the proportionality into a real value of LOL, therefore results of equation 2 will be titled as  $LOL^*$  and the constant will depend on fuel used. In this study, the constant corresponds to slope obtained for the linear fit (dashed line) of each fuel.

The correlation shows that LOL decreases with increasing ambient temperature and density, as it reduces the amount of air required to burn the fuel injected. Besides, LOL increases with increasing injection pressure, as a higher injection velocity moves the reaction stabilization region [31], [32], [36]. In addition, fuel density appears implicitly in the correlation, so that the lower the fuel density, the higher the LOL should be.

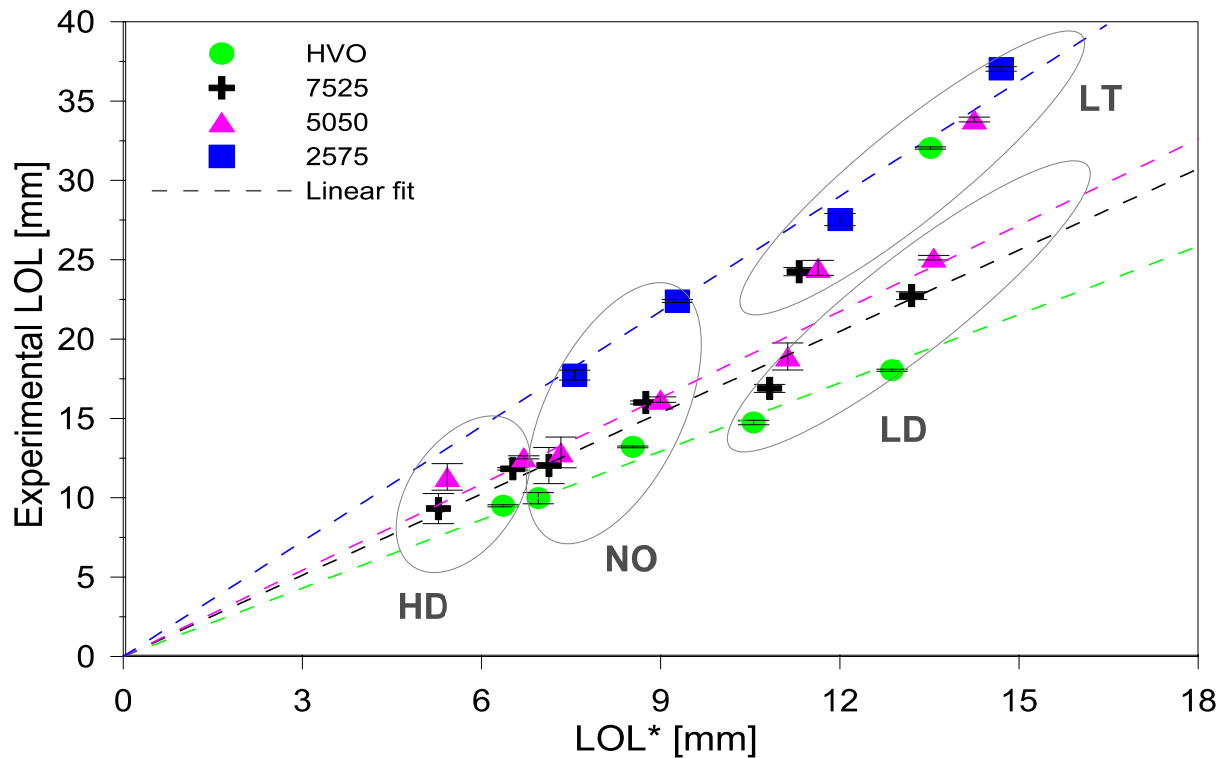


Figure 8. Comparison of current experimental  $LOL^*$  data with correlations by Benajes [32] for each blend and operating condition.

According to this, the shortest LOL should be obtained for HVO while increasing as LPG ratio in the blend increases. In this sense, experimental results show a stratification by fuels and by operating conditions, as it is represented in Figure 8. Operating conditions are represented with ellipses in continuous lines. A similar behaviour to the one described by equation 2 is observed also with experimental data.

For  $15.2 \text{ kg/m}^3$  and  $22.8 \text{ kg/m}^3$  ambient density, the difference of LOL between HVO-LPG blends and pure HVO was around 15 and 30%, while at  $30.4 \text{ kg/m}^3$  the difference is still between 12% and 36%. For the LT condition, the observed differences are only between 5% and 15%. Besides, as it was observed for ID, these points show larger LOL values than the equation 2 would predict for all the blends.

### 3.2 Soot Formation

A brighter flame can be the consequence of either higher temperature in the flame, higher soot concentration, or both. However, natural flame luminosity has been used previously in the literature [28] for qualitative analysis of soot formation. For this reason, natural luminosity has been considered of interest for the analysis of soot formation behavior of the different fuels tested. On the assumption that fuels have similar flame temperature, the differences of luminosity only correspond to formed soot. Additionally, in previous work, the relationship between flame temperature and soot concentration has been studied and it was determined that both parameters are not directly linked and the higher flame temperature is not the governing factor for higher soot production [37].

High-speed flame emission images are presented in Figure 9, and show temporal evolution of natural luminosity for each fuel. From left to right, percentage of LPG increases. It is possible to observe that light radiation reduces significantly with the increase of LPG ratio, even when the LPG proportion is the lowest (second column from left to right). The first instant of time shown (1.5 ms) corresponds to a time in which the combustion has started for all the blends. At this time, HVO has the highest light intensity. On the other hand, the flame of 2575 can hardly be seen. In addition, at 3.5 ms (third row of the Figure 9 seen from top to bottom) the difference in brightness is still very marked, as well as the flames are already developed for all fuels.

Considering the flames produced by the LPG, the maximum intensity levels are not reached (red color) compared to HVO. This can be explained by the fact that these blends start the combustion later than the HVO. Also, these blends have their flame lift off at longer distance from the injector, and as was studied in [37], LOL is a governing factor for soot production. Longer LOL allows more air entrainment as it was discussed previously. For blends 7525 and 5050 is not clear which flame has higher luminosity. This can be explained by the fact that the

difference between ID and LOL is not significant either. But what is quite clear is that adding LPG favors the reduction of luminosity and therefore the soot formation will be reduced.

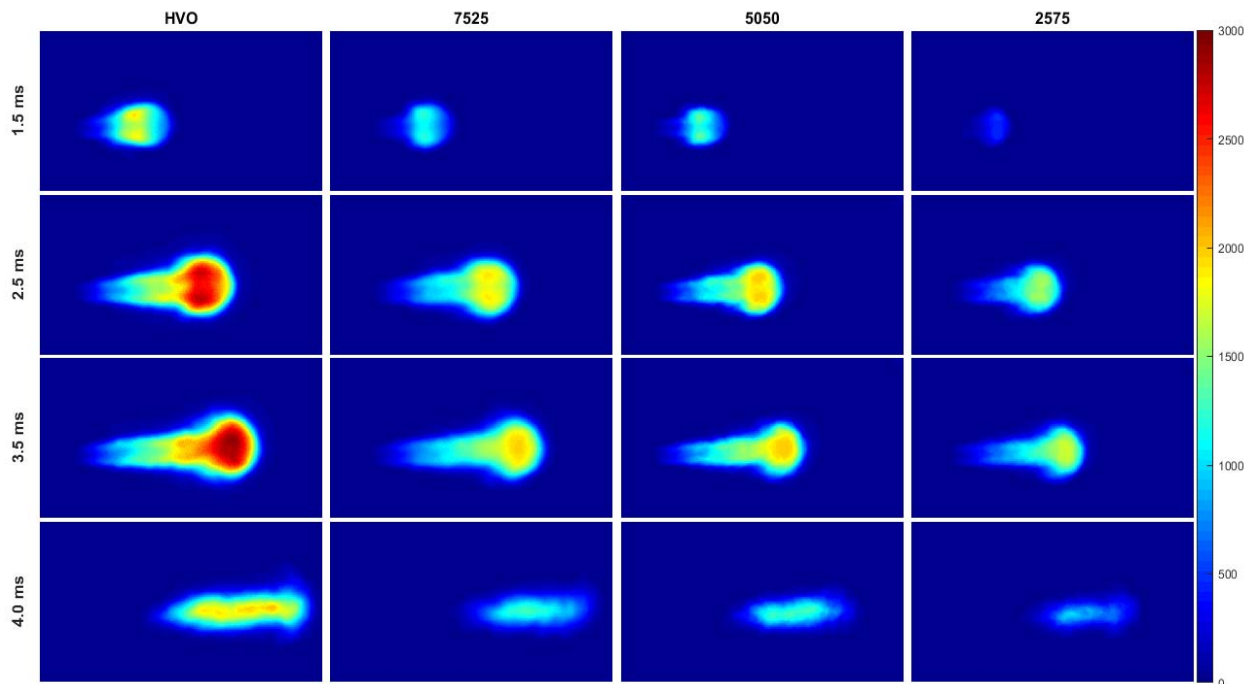


Figure 9. Mean soot formation for all fuels at 900K,  $\rho=22.8 \text{ kg/m}^3$  NO and 500 bar of injection pressure.

In order to quantify the intensities in each fuel and make evident the effect of the addition of LPG, the values shown in Figure 10 correspond to the mean intensity of the flame for all the fuels, at a certain instant, where the flame is stabilized, i. e. 3.5 ms after start of injection. In this figure, the two injection pressures and all the operating condition have been represented. It is possible to observe that adding LPG reduces the luminosity of the flame around 30% when the percentage of LPG in the mixture is the minimum tested (blend 7525). Additionally, during low temperature condition the luminosity observed for all fuels were quite small. As a consequence, the results are less accurate because it is difficult to detect the low flame intensity as the light radiation could be mistaken for the background noise of the images. And for that

reason was not included in the analysis. Figure 10 shows that increasing the injection pressure also reduces the intensity of the flame, as consequence of LOL increment. It is also possible to appreciate that when the density increases, the luminosity also increases. Xuan et al. in [37] indicates that a shorter Lift-off Length (larger  $\phi$ ) has higher effect in the soot precursors than flame temperature which would result in a faster soot rise in the flame. Figure 10 shows that, in general, differences between HD and NO operating condition are below or close to the standard deviation (represented by the error bars) which represents experimental variability. Thus, it is difficult to confirm the behavior described above between these two operating conditions. .

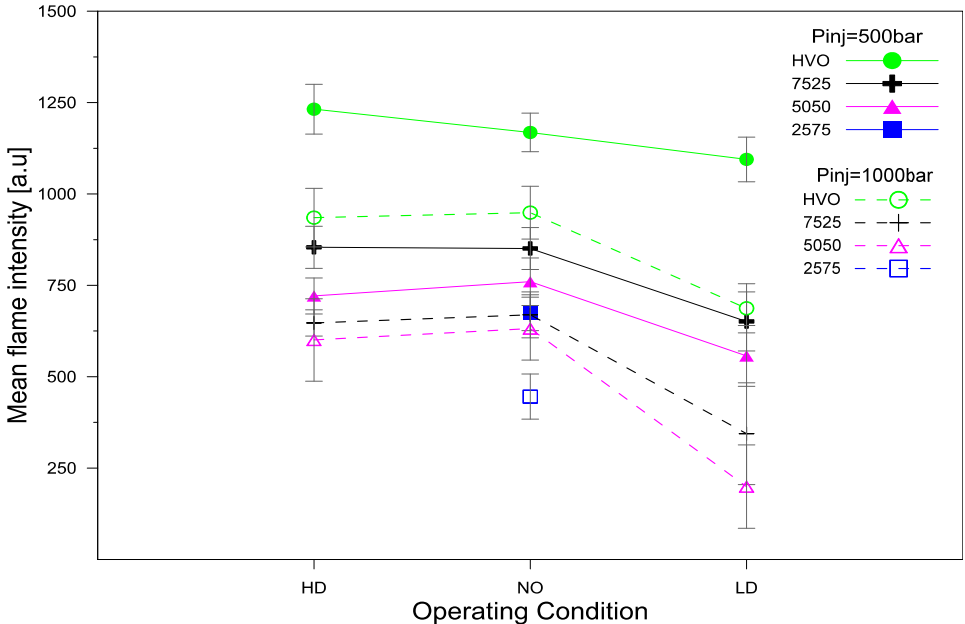


Figure 10. Mean light intensity in the spray for all conditions at two injection pressure at 3.2 ms ASOI.

It is worth mentioning that blends with LPG have bigger ID and longer LOL than pure HVO. High values of both parameters favour less soot formation as more air is entrained and a better mixing is achieved upstream of the flame, which stabilizes at longer distances from the nozzle. This statement is supported by the calculations of the equivalence fuel-air ratio at the spray axis, spray radius and Lift-off distance performed with a 1D spray model (DICOM) which is

widely described in [38]. In DICOM the spray is assumed to be injected into a quiescent air volume, large enough so that the injected fuel does not change the conditions far away from the injector tip. The fuel stream has a uniform velocity profile at the tip of the nozzle. This flow exchanges its momentum with the ambient, and sets it moving. As a result of this, the spray increases its width with its axial distance. This phenomenon is modeled with two spray angles (one for the near-field and other angle for the far-field), with a transition occurring at a determined distance from the orifice. These parameters are inputs to the model as well as the fuel or blend composition, nozzle diameter, nozzle injection conditions (mass and momentum fluxes), and ambient condition (pressure, temperature, density and oxygen concentration). All these inputs come from the experiments. The outputs are the jet spray tip penetration as well as the mixture field at every simulated time instant. Other input is the spray cone angle that it is adjusted from comparison between penetration made by DICOM and the experimental penetration. In the current work, for HVO was used dodecane as surrogate while for LPG a blend of butane and propane was defined, according to the technical data sheet provided by supplier. Then blends were set according to the mass fraction used in the experimental tests: 25%, 50% and 75% of LPG. The output is the air/fuel mixture field at every simulated time instant.

Table 3. Equivalence fuel air ratio at LOL at NO operating condition and 1000 bar of injection pressure

<b>Fuel</b>	<b>LOL [mm]</b>	<b><math>\Phi</math> at spray axis</b>
<b>HVO</b>	13.21	<b>9.41</b>
<b>7525</b>	16.00	<b>7.05</b>
<b>5050</b>	16.18	<b>6.74</b>
<b>2575</b>	22.4	<b>3.93</b>

To give a better understanding about effect of LPG on soot formation, Table 3 represents the values of equivalent fuel-air ratio ( $\Phi$ ) at lift-off length at the spray axis when the flame is stabilized (3200  $\mu$ s). Results correspond to NO at 1000 bar of injection pressure. The tendency is representative for the rest of operating condition. It is observed that an important difference of  $\Phi$  between HVO and HVO-LPG blends exists. The larger LOL as LPG content increases means also more air when reactions start which explains the lower soot formed by them.

#### **4 Conclusions**

Effects of HVO-LPG blend ratio over combustion development were investigated using three optical techniques. Tests were carried out in a constant pressure vessel and a dedicated injection system was implemented to inject the mixture of HVO and LPG at the same time. Combustion characteristics were analyzed at different ambient densities, temperatures, and injection pressures. The main conclusions of this work are summarized as follows:

- The injection system implemented has shown a stable behavior, even when increasing LPG content. Spray penetration results suggest that no difference should be expected in terms of mass flow rate or spray momentum flux for the different blends used in this work.
- Ignition delay increases with the LPG content in the blend indicating that it acts as an ignition inhibitor of HVO. The sensitivity of the different blends to operation conditions was evaluated. For 25% and 50% LPG ratios, similar behavior was observed while larger differences were found when increasing LPG content to 75%.
- Flame Lift off Length increases when increasing proportion of LPG. According with the correlation utilized, experimental results present similar variations as the ones predicted for different blend densities. As it was observed for ID, 25% and 50% LPG

blends present a similar behavior while larger differences are observable for 75% LPG blend.

- The flame luminosity for blends is smaller than for pure HVO, and it decreases when increasing LPG content. This can be related to less soot formation, as a consequence of more air entrainment due to larger ID and LOL.

## References

- [1] Roadmap to a Single European Transport Area – Towards a competitive and resource efficient transport system. White Paper, COM(2011) 144 final.
- [2] J. Sheehan, V. Camobreco, J. Duffield, M. Graboski, H. Shapouri, An Overview of Biodiesel and Petroleum Diesel Life Cycles, NREL/TP-580-24772 .
- [3] M.M. Hasan, M.M. Rahman, Performance and emission characteristics of biodiesel–diesel blend and environmental and economic impacts of biodiesel production: A review, *Renew. Sustain. Energy Rev.* 74 (2017) 938–948.  
doi:10.1016/j.rser.2017.03.045.
- [4] O.P. Bhardwaj, A.F. Kolbeck, T. Kkoerfer, M. Honkanen, Potential of Hydrogenated Vegetable Oil (HVO) in Future High Efficiency Combustion System, *SAE Int. J. Fuels Lubr.* 6 (2013) 157–169. doi:10.4271/2013-01-1677.
- [5] A. Chakraborty, S. Roy, R. Banerjee, An experimental based ANN approach in mapping performance-emission characteristics of a diesel engine operating in dual-fuel mode with LPG, *J. Nat. Gas Sci. Eng.* 28 (2016) 15–30. doi:10.1016/j.jngse.2015.11.024.
- [6] H. Aatola, M. Larmi, T. Sarjovaara, S. Mikkonen, Hydrotreated Vegetable Oil (HVO) as a Renewable Diesel Fuel: Trade-off between NO<sub>x</sub>, Particulate Emission, and Fuel Consumption of a Heavy Duty Engine, *SAE Int J Engines.* 1 (2008) 1251–1262.  
doi:10.4271/2008-01-2500.



- [7] Hydrotreated vegetable oil, premium renewable biofuel for diesel engines. Neste Oil. February 2014.pdf, (n.d.).
- [8] D. Singh, K.A. Subramanian, R. Bal, S.P. Singh, R. Badola, Combustion and emission characteristics of a light duty diesel engine fueled with hydro-processed renewable diesel, *Energy*. 154 (2018) 498–507. doi:10.1016/j.energy.2018.04.139.
- [9] W. Zhong, T. Pachiannan, Z. He, T. Xuan, Q. Wang, Experimental study of ignition, lift-off length and emission characteristics of diesel/hydrogenated catalytic biodiesel blends, *Appl. Energy*. 235 (2019) 641–652. doi:10.1016/j.apenergy.2018.10.115.
- [10] H.S. Tira, J.M. Herreros, A. Tsolakis, M.L. Wyszynski, Influence of the addition of LPG-reformate and H<sub>2</sub> on an engine dually fuelled with LPG–diesel, –RME and –GTL Fuels, *Fuel*. 118 (2014) 73–82. doi:10.1016/j.fuel.2013.10.065.
- [11] S. Goto, D. Lee, J. Shakal, N. Harayama, F. Honjyo, H. Ueno, Performance and Emissions of an LPG Lean-Burn Engine for Heavy Duty Vehicles, SAE Tech Pap, 1999. doi.org/10.4271/1999-01-1513.
- [12] M.M. Musthafa, A comparative study on coated and uncoated diesel engine performance and emissions running on dual fuel (LPG – biodiesel) with and without additive, *Ind. Crops Prod*. 128 (2019) 194–198. doi:10.1016/j.indcrop.2018.11.012.
- [13] K K. Hashimoto, H. Ohta, T. Hirasawa, M. Arai, M. Tamura, Evaluation of Ignition Quality of LPG with Cetane Number Improver, SAE Tech. Pap, 2002. doi:10.4271/2002-01-0870.
- [14] J. Benajes, S. Molina, A. García, J. Monsalve-Serrano, Effects of low reactivity fuel characteristics and blending ratio on low load RCCI (reactivity controlled compression ignition) performance and emissions in a heavy-duty diesel engine, *Energy*. 90 (2015) 1261–1271. doi:10.1016/j.energy.2015.06.088.

- [15] J. Benajes, A. García, J. Monsalve-Serrano, V. Boronat, Dual-Fuel Combustion for Future Clean and Efficient Compression Ignition Engines, *Appl. Sci.* 7 (2016) 36. doi:10.3390/app7010036.
- [16] J. Benajes, A. García, J. Monsalve-Serrano, V. Boronat, Achieving clean and efficient engine operation up to full load by combining optimized RCCI and dual-fuel diesel-gasoline combustion strategies, *Energy Convers. Manag.* 136 (2017) 142–151. doi:10.1016/j.enconman.2017.01.010.
- [17] S.L. Kokjohn, R.M. Hanson, D.A. Splitter, R.D. Reitz, Fuel reactivity controlled compression ignition (RCCI): a pathway to controlled high-efficiency clean combustion, *Int. J. Engine Res.* 12 (2011) 209–226. doi:10.1177/1468087411401548.
- [18] R. Payri, J. Gimeno, M. Bardi, A.H. Plazas, Study liquid length penetration results obtained with a direct acting piezo electric injector, *Appl. Energy.* 106 (2013) 152–162. doi:10.1016/j.apenergy.2013.01.027.
- [19] J. Gimeno, P. Martí-Aldaraví, M. Carreres, J.E. Peraza, Effect of the nozzle holder on injected fuel temperature for experimental test rigs and its influence on diesel sprays, *Int. J. Engine Res.* 19 (2018) 374–389. doi:10.1177/1468087417751531.
- [20] J.V. Pastor, J.M. García-Oliver, A. García, C. Micó, S. Möller, Application of optical diagnostics to the quantification of soot in n -alkane flames under diesel conditions, *Combust. Flame.* 164 (2016) 212–223. doi:10.1016/j.combustflame.2015.11.018.
- [21] J J. Pastor, J.M. Garcia-Oliver, A. Garcia, V.R. Nareddy, Characterization of Spray Evaporation and Mixing Using Blends of Commercial Gasoline and Diesel Fuels, *SAE Tech. Pap, Engine-Like Conditions*, in: 2017. doi:doi:10.4271/2017-01-0843.
- [22] G.S. Settles, *Schlieren and Shadowgraph Techniques: Visualizing Phenomena in Transparent Media*, Springer Science & Business Media, 2012.

- [23] J.V. Pastor, R. Payri, J.M. Garcia-Oliver, F.J. Briceño, Schlieren Methodology for the Analysis of Transient Diesel Flame Evolution, *SAE Int. J. Engines*. 6 (2013) 1661–1676. doi:10.4271/2013-24-0041.
- [24] D.L. Siebers, Liquid-Phase Fuel Penetration in Diesel Sprays, in: *SAE Tech. Pap.*, 1998. doi:10.4271/980809.
- [25] Engine Combustion Network | Engine Combustion Network Website, (n.d.). <https://ecn.sandia.gov/> (accessed May 2, 2019).
- [26] J.M. Desantes, J.V. Pastor, J.M. García-Oliver, F.J. Briceño, An experimental analysis on the evolution of the transient tip penetration in reacting Diesel sprays, *Combust. Flame*. 161 (2014) 2137–2150. doi:10.1016/j.combustflame.2014.01.022.
- [27] R. Payri, J.P. Viera, Y. Pei, S. Som, Experimental and numerical study of lift-off length and ignition delay of a two-component diesel surrogate, *Fuel*. 158 (2015) 957–967. doi:10.1016/j.fuel.2014.11.072.
- [28] J.V. Pastor, J.M. Garcia-Oliver, A. Garcia, M. Pinotti, Soot Characterization of Diesel/Gasoline Blends Injected through a Single Injection System in CI engines, in: *SAE Tech. Pap.*, 2017. doi:10.4271/2017-24-0048.
- [29] M. Reyes, F.V. Tinaut, B. Giménez, J.V. Pastor, Effect of hydrogen addition on the OH\* and CH\* chemiluminescence emissions of premixed combustion of methane-air mixtures, *Int. J. Hydrog. Energy*. 43 (2018) 19778–19791. doi:10.1016/j.ijhydene.2018.09.005.
- [30] D. Siebers, B. Higgins, Flame Lift-Off on Direct-Injection Diesel Sprays Under Quiescent Conditions, *SAE Tech Pap*, 2001. doi.org/10.4271/2001-01-0530.

- [31] J. Benajes, R. Payri, M. Bardi, P. Martí-Aldaraví, Experimental characterization of diesel ignition and lift-off length using a single-hole ECN injector, *Appl. Therm. Eng.* 58 (2013) 554–563. doi:10.1016/j.applthermaleng.2013.04.044.
- [32] R. Payri, F.J. Salvador, J. Manin, A. Viera, Diesel ignition delay and lift-off length through different methodologies using a multi-hole injector, *Appl. Energy*. 162 (2016) 541–550. doi:10.1016/j.apenergy.2015.10.118.
- [33] S. Kook, L.M. Pickett, Liquid length and vapor penetration of conventional, Fischer–Tropsch, coal-derived, and surrogate fuel sprays at high-temperature and high-pressure ambient conditions, *Fuel*. 93 (2012) 539–548. doi:10.1016/j.fuel.2011.10.004.
- [34] R. Payri, J.M. García-Oliver, T. Xuan, M. Bardi, A study on diesel spray tip penetration and radial expansion under reacting conditions, *Appl. Therm. Eng.* 90 (2015) 619–629. doi:10.1016/j.applthermaleng.2015.07.042.
- [35] R. Payri, J.P. Viera, V. Gopalakrishnan, P.G. Szymkowicz, The effect of nozzle geometry over ignition delay and flame lift-off of reacting direct-injection sprays for three different fuels, *Fuel*. 199 (2017) 76–90. doi:10.1016/j.fuel.2017.02.075.
- [36] L.M. Pickett, D.L. Siebers, C.A. Idicheria, Relationship Between Ignition Processes and the Lift-Off Length of Diesel Fuel Jets, *SAE Tech Pap*, 2005. doi.org/10.4271/2005-01-3843.
- [37] T. Xuan, J.M. Desantes, J.V. Pastor, J.M. Garcia-Oliver, Soot temperature characterization of spray a flames by combined extinction and radiation methodology, *Combust. Flame*. 204 (2019) 290–303. doi:10.1016/j.combustflame.2019.03.023.
- [38] J.M. Desantes, J.V. Pastor, J.M. García-Oliver, J.M. Pastor, A 1D model for the description of mixing-controlled reacting diesel sprays, *Combust. Flame*. 156 (2009) 234–249. doi:10.1016/j.combustflame.2008.10.008.